International Journal of Thermophysics, Vol. 23, No. 3, May 2002 (© 2002)

Thermodynamic Properties of HFC-227ea

V. A. Gruzdev,[1] R. A. Khairulin,[1] S. G. Komarov,[1] and S. V. Stankus[1, 2]

Received May 1, 2001

The density and speed of sound in gaseous and liquid 1,1,1,2,3,3,3-heptafluoropropane (HFC-227ea) have been studied by a γ-attenuation technique, an ultrasonic interferometer, and an isochoric piezometer method over the temperature range of 273 to 383 K at pressures up to 3.5 MPa. The purity of the samples used throughout the measurements are 99.99 mol%. The pressures of the saturated vapor were measured over the same temperature range. The experimental uncertainties of the temperature, pressure, density, and speed of sound measurements were estimated to be within ± 20 mK, ± 1.5 kPa, $\pm 0.2\%$, and $\pm(0.15–0.2)\%$, respectively. On the basis of the obtained data, the isobaric molar heat capacity of HFC-227ea was calculated for the ideal-gas state.

KEY WORDS: density; gamma densitometer; HFC-227ea; isochoric piezometer; speed of sound; ultrasonic interferometer; vapor pressure.

1. INTRODUCTION

Fluorinated derivatives of propane (HFC) are currently considered as alternative ecologically safe working substances for refrigerating equipment, air conditioning, and heat conversion. Unfortunately, physical and chemical properties of these substances have not been well studied. An overview of experimental data on the thermophysical properties of HFC-227ea which have been carried out to the present day are given in Refs. 1 and 2. The available results are not comprehensive and require independent checks. Moreover, the measurements were conducted partly on lower purity samples and within narrow intervals of temperature and pressure.

[1] Institute of Thermophysics, Siberian Branch of Russian Academy of Sciences, Lavrentyev Ave., 1, Novosibirsk 630090, Russia.

[2] To whom correspondence should be addressed. E-mail: stankus@itp.nsc.ru

0195-928X/02/0500-0809/0 © 2002 Plenum Publishing Corporation

In the present paper, we report measurements for the saturated vapor pressure, density, and speed of sound in liquid and gaseous 1,1,1,2,3,3,3-heptafluoropropane (HFC-227ea) over the temperature range of 273 to 383 K and at pressures up to 3.5 MPa. The purity of the samples used throughout the measurements was 99.99 mol%. On the basis of the obtained data, the isobaric molar heat capacity of HFC-227ea was calculated for the ideal-gas state.

2. EXPERIMENTAL

A cylindrical stainless steel isochoric piezometer of $(438.86 \pm 0.15)\ \mathrm{cm}^3$ capacity was used for the measurement of the vapor density and the saturated vapor pressure. The cell was immersed in a thermostatic bath. The temperature in the bath was held to within ± 10 mK throughout the measurements. The temperature of the piezometer was measured with a 10 Ω platinum resistance thermometer. The uncertainty in the temperature measurement was estimated to be ± 0.02 K. The pressure was measured by means of piston gauges (MP-6, MP-60) and by a vacuum gage of the VO-1227 type using a membrane null indicator with an uncertainty of 0.05 and 0.25%, respectively. The instrumental error in the pressure measurement in the range of up to 0.2 MPa did not exceed 0.2 kPa, and at 3.5 MPa it was about 1.5 kPa. The main contribution to the error of the vapor density determination gives an uncertainty in the sample mass of $(0.01\text{–}0.05) \times 10^{-3}$ kg. It results from adsorption and residual vapor in the piezometer after freezing of HFC-227ea in a vessel for weighing. The saturated vapor pressure (P_s) was measured directly in the piezometer after holding the sample at a constant temperature for two hours.

The speed of sound was measured by an ultrasonic interferometer fabricated from stainless steel with lithium niobate transducers operated in the frequency range of 1.15 to 1.16 MHz. Instrumental errors of the pressure and temperature measurements were the same as in the vapor density experiments. A detailed description of the measurement method and the experimental setup has been given in previous publications [3, 4]. To estimate the instrumental error in the measurements of the speed of sound, we made performance test measurements in pure argon. The results obtained during these experiments differ from the most reliable data by no more than 0.06%.

The investigation of the density in the liquid state was performed by irradiating the samples with a narrow beam of gamma quanta from a ^{137}Cs source (220 GBq). Details of the experimental equipment and procedures have been described elsewhere [5].

The HFC-227ea sample was supplied by the Russian Scientific Center "Applied Chemistry" (St. Petersburg) with a stated minimum purity of 99.99 mol per cent. Before the experiments, the initial product was purified removing water and volatile components. For this purpose, HFC-227ea was kept in a supply reservoir filled with silica gel that had been activated at 393 K. Then, it was passed into another, preliminary evacuated vessel (thermal compressor), where it was cooled by liquid nitrogen and purified removing low-molecular-mass components by long evacuation followed by cyclic remelting of the sample.

3. RESULTS AND DISCUSSION

3.1. Saturated Vapor Pressure

The results of the measurements for the saturated vapor pressure are given in Table I. The experimental data were approximated by two empirical equations for the liquid-vapor equilibrium curve:

$$\ln(P_s) = C_0 + \frac{C_1}{T} + C_2 \ln(T) + C_3 T + C_4 T^2 \tag{1}$$

where $C_0 = -105.87983$, $C_1 = -1752.8459$, $C_2 = 26.23416$, $C_3 = -0.1347143$, $C_4 = 9.646847 \times 10^{-5}$, P_s is the vapor pressure in kPa, T is the temperature in K, and

$$\ln\left(\frac{P_s}{P_0}\right) = (C_0 + C_1\varepsilon + C_2\varepsilon^{1.25} + C_3\varepsilon^3 + C_4\varepsilon^7)\frac{T_c}{T} \tag{2}$$

where $C_0 = 0.0001295051$, $C_1 = -8.1458345$, $C_2 = 1.586356$, $C_3 = -2.838342$, $C_4 = -71.35186$, $\varepsilon = 1 - T/T_c$, $T_c = 375.95$ K is the critical

Table I. Experimental Vapor Pressure of HFC-227ea

T (K)	P (kPa)	T (K)	P (kPa)	T (K)	P (kPa)	T(K)	P (kPa)
272.60	192.21	282.82	277.20	298.18	457.0	323.15	915.7
272.95	196.54	286.92	318.50	303.15	530.5	323.15	917.8
275.92	215.16	286.92	319.20	303.16	530.0	333.15	1176.7
278.06	234.68	290.49	360.80	312.15	682.6	343.15	1486.7
278.30	234.09	293.15	390.30	313.13	701.0	353.15	1856.8
282.79	277.20	293.15	391.40	313.15	703.0	363.15	2295.2
282.81	277.21	293.15	390.06	321.15	870.8	365.02	2392.5
282.82	277.27	293.15	392.70	322.15	892.8	373.15	2818.1

temperature [2, 6], and $P_0 = 2987.7$ kPa is a reference pressure that is close to the critical pressure [2]. The standard deviations are practically the same for both equations, namely ~ 1.5 kPa (0.37%). The maximum deviations (at 365.02 K) are 4.00 and 4.92 kPa for Eqs. (1) and (2), respectively. Equation (1) is preferred when the experimental values of critical parameters are unknown. Equation (2) can be transformed into

$$\ln\left(\frac{P_s}{P_c}\right) = (C_1^*\varepsilon + C_2\varepsilon^{1.25} + C_3\varepsilon^3 + C_4\varepsilon^7)\frac{T_c}{T} \qquad (2^*)$$

where $P_c = P_0 \exp(C_0) = 2988.1$ kPa is the critical pressure, $C_1^* = C_1 + C_0 = -8.145705$, and the parameters C_2, C_3, C_4 are the same as for Eq. (2). The critical pressure (2988.1 kPa) at the critical temperature $T_c = 375.95$ K obtained from Eqs. (2) and (2*) are in good agreement with $P_c = 2987.7$ kPa [2]. Substitution of the values of the critical temperature $T_c = 376.65$ K [7], and $T_c = 375.95$ K [6, 8] into Eq. (1) gives $P_c = 3025.6$ kPa, and $P_c = 2983.6$ kPa, respectively. The latter value is only about 4.1 kPa lower than published data [2]. The normal boiling temperature T_b was determined by extrapolating Eq. (1) to the pressure 101.325 kPa. The obtained value $T_b = 256.84 \pm 0.2$ K agrees with data [2, 9] within the estimated error. Figure 1 shows the results of our measurements in comparison with data

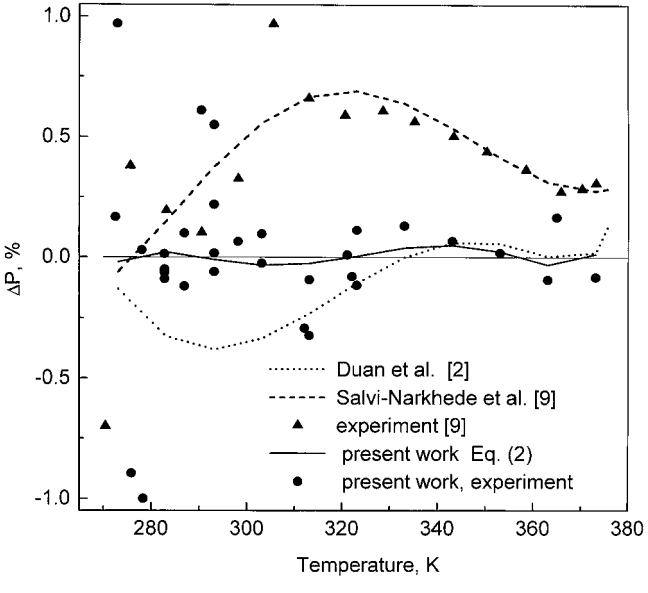

Fig. 1. Deviations of the saturated vapor pressure from Eq. (1), as a function of temperature; $\Delta P = 100[P(\text{Ref.})/P(\text{Eq. (1)}) - 1]$.

[2, 9]. As is seen from the figure, the discrepancies between Eqs. (1) and (2) are within the standard deviations. The data of Ref. 2 lie lower by about 0.2 to 0.3% in the temperature range from 280 to 320 K, whereas the data of Ref. 9 lie higher by about 0.25 to 0.5% than those calculated from Eq. (1) at temperatures above 300 K.

3.2. Vapor Density

P, ρ, T-properties of HFC-227ea in the vapor phase were measured on eight quasi-isochores (at constant mass of the substance in a piezometer) over the temperature range from 313.15 to 383.15 K and pressure range from 690 to 3185 kPa. The uncertainties of the temperature, pressure, and specific volume did not exceed ± 0.02 K, 1.5 kPa, and $\pm 0.15\%$, respectively. The experimental data reduced to a constant density are given in Table II. Corrections to the measured vapor pressure are due to thermal expansion

Table II. Experimental Vapor Density (ρ_g) of HFC-227ea

T (K)	P (kPa)	T (K)	P (kPa)	T (K)	P (kPa)
$\rho_g = 55.102\ \text{kg}\cdot\text{m}^{-3}$		$\rho_g = 152.93\ \text{kg}\cdot\text{m}^{-3}$		$\rho_g = 220.22\ \text{kg}\cdot\text{m}^{-3}$	
313.15	690.14	351.15	1723.50	362.15	2203.62
315.15	697.19	352.15	1735.80	362.33	2204.72
323.15	727.54	353.15	1747.30	363.15	2223.90
333.15	761.74	363.15	1866.07	364.15	2237.70
$\rho_g = 72.987\ \text{kg}\cdot\text{m}^{-3}$		373.15	1979.73	373.15	2400.38
323.15	899.14	383.15	2092.24	383.15	2573.78
325.15	908.93	$\rho_g = 196.35\ \text{kg}\cdot\text{m}^{-3}$		$\rho_g = 359.58\ \text{kg}\cdot\text{m}^{-3}$	
333.15	947.73	363.15	2105.60	373.15	2818.12
343.15	994.96	363.17	2105.57	374.15	2857.40
353.15	1041.40	373.14	2267.66	374.15	2857.30
363.15	1086.80	373.15	2267.76	375.61	2912.30
373.15	1131.37	383.15	2421.66	375.62	2912.70
383.20	1175.86	$\rho_g = 272.33\ \text{kg}\cdot\text{m}^{-3}$		379.22	3043.83
$\rho_g = 91.979\ \text{kg}\cdot\text{m}^{-3}$		367.30	2468.12	383.15	3185.00
333.15	1116.42	368.15	2491.02		
335.15	1129.98	369.15	2518.61		
338.15	1149.62	369.15	2515.21		
343.15	1182.86	371.15	2568.39		
353.15	1244.75	373.15	2617.10		
363.15	1304.05	373.59	2629.60		
373.15	1363.79	383.15	2859.54		
383.15	1422.10				

Table III. Parameters of Eq. (3)

ρ (kg·m^{-3})	T range (K)	C_0	C_1	C_2	C_3	SD (%)
72.95	323.15–383.15	1.055306	−0.222922	0.210518	−0.312530	0.01
91.979	333.15–383.15	1.187151	−0.956790	1.386539	−0.964853	0.05
152.93	351.15–383.15	1.089244	−0.325507	0.291392	−0.589321	0.02
196.35	363.15–383.15	1.584860	−3.070861	4.785751	−3.033457	0.004
220.22	362.15–383.15	1.210626	−0.845057	0.862544	−0.945680	0.07
272.33	367.27–383.15	1.875826	−4.547584	7.132775	−4.432237	0.05
359.58	373.15–383.15	2.581479	−8.251668	13.23693	−7.839136	0.02

and pressure deformation of the piezometer and do not exceed $\pm 0.2\%$. The experimental data for each isochore were fitted by the equation,

$$z_i(T) = C_0 + C_1 t + C_2 t^2 + C_3 t^3 \tag{3}$$

where $t = 300/T$, $z_i = \mu P/(RT\rho_g)$ is the compressibility factor, ρ_g (kg·m^{-3}) is the vapor density for ith isochore, $R = 8.31447\ \mathrm{J \cdot mol^{-1} \cdot K^{-1}}$ is the universal gas constant, and $\mu = 0.17003\ \mathrm{kg \cdot mol^{-1}}$ is the molar mass of 1,1,1,2,3,3,3-heptafluoropropane. To improve the extrapolation performance of Eq. (3), it was assumed that $z_i = 1$ at a temperature near Boyle's temperature T_B. The value of T_B was estimated using the relation $T_B \sim 2.8T_C$ [10]. The coefficients of Eq. (3) and the standard deviations (SD) of the experimental data are given in Table III. To determine virial coefficients, smoothed data for the compressibility factor were fitted by the polynomial,

$$(z-1)/d_g = B + Cd_g + Dd_g^2 \tag{4}$$

where $d_g = 0.001\rho_g/\mu$ is the vapor density in mol·l^{-1}, and B, C, and D are the experimental second, third, and forth virial coefficients, respectively. The values of the coefficients B, C, and D are given in Table IV. The

Table IV. Experimental Virial Coefficients for HFC-227ea

T (K)	B (l·mol^{-1})	C (l^2·mol^{-2})	D (l^3·mol^{-3})
343.15	−0.46482 ± 0.0027	0.0617 ± 0.0046	
353.15	−0.42593 ± 0.0047	0.04931 ± 0.006	
363.15	−0.39715 ± 0.003	0.04918 ± 0.0036	
373.15	−0.37044 ± 0.0045	0.04675 ± 0.0085	0.000282 ± 0.003
383.15	−0.34618 ± 0.005	0.04368 ± 0.01	0.00078 ± 0.004
393.15	−0.32289 ± 0.007	0.03968 ± 0.015	0.00139 ± 0.005

deviations of our experimental data, as well as literature values from Eq. (4) are shown in Fig. 2. Our data are in good agreement with the results of Duan et al. [2] and Patek et al. [11]. The P, ρ, T-data calculated by Benedetto et al. [1] on the basis of the acoustic measurements and a simple model for the second virial coefficient differ significantly from others.

The saturated-vapor densities were determined by extrapolation of Eqs. (3) and (4) to the coexistence curve. The data were fitted by the equation,

$$\rho_g = 584(1 + C_1\varepsilon^{0.345} + C_2\varepsilon + C_3\varepsilon^{2/3} + C_4\varepsilon^{4/3}) \tag{5}$$

where $C_1 = -1.89027$, $C_2 = -0.13669367$, $C_3 = -0.0265417$, $C_4 = 1.5988818$, and $T_c = 376.65$ K is the critical temperature [7]. Equation (5) describes the experimental data with a standard deviation of $\pm 3\,\mathrm{kg \cdot m^{-3}}$ in the temperature range from 313.15 to 373.15 K.

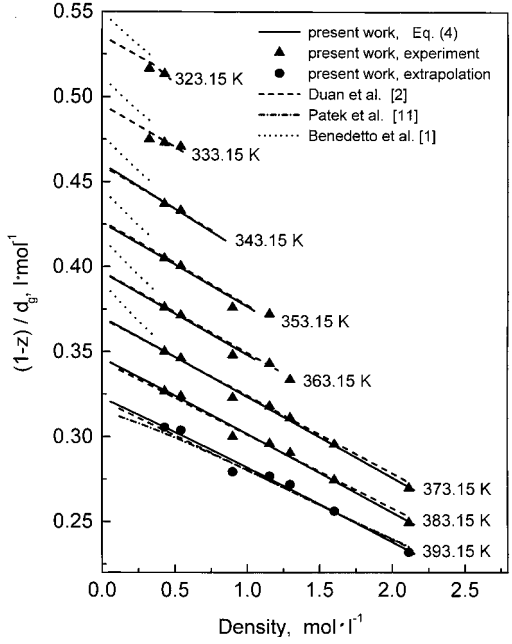

Fig. 2. Comparison of $P\rho T$-data for HFC-227ea. z is the compressibility factor; d_g is the vapor density.

3.3. Liquid Density

The results of liquid density (ρ_l) measurements are given in Table V. The data along the coexistence curve were fitted using Eq. (5) with $C_1 = 1.1331943$, $C_2 = -8.203351$, $C_3 = 5.052361$, and $C_4 = 5.21300$, with a standard deviation equal to 1.06 $kg \cdot m^{-3}$ (0.092%) and a maximum deviation (at 312.3 K) equal to 1.49 $kg \cdot m^{-3}$. Comparisons of our data and the results of other researchers [8, 12, 13] for HFC-227ea are shown in Fig. 3. (The results of Salvi et al. [9] lie significantly higher and are not shown in Fig. 3.)

The shape of the liquid-vapor coexistence curve on a T-ρ phase diagram made with our data is shown in Fig. 4. The temperature dependence of the midpoints of the coexistence curve $\rho_d = (\rho_l + \rho_g)/2$ obeys the classical law

Table V. Experimental Liquid Density of HFC-227ea

T (K)	P (kPa)	ρ_l ($kg \cdot m^{-3}$)	T (K)	P (kPa)	ρ_l ($kg \cdot m^{-3}$)
296.99	905.08	1394.3	353.24	1891.0	1084.2
303.27	905.08	1368.0			
312.96	905.08	1324.1	298.15	2355.5	1400.0
318.15	905.08	1296.8	305.58	2355.5	1371.0
322.12	905.08	1277.5	312.54	2355.5	1340.1
322.55	905.08	1273.5	320.08	2355.5	1306.1
322.89	905.08	1272.4	327.27	2355.5	1272.0
323.40	905.08	1268.3	334.48	2355.5	1234.0
			341.77	2355.5	1189.5
297.81	1516.4	1395.9	347.93	2355.5	1149.8
303.58	1516.4	1371.9	352.73	2355.5	1112.2
311.78	1516.4	1336.0	357.58	2355.5	1066.0
317.94	1516.4	1306.8	360.58	2355.5	1034.6
325.40	1516.4	1268.9	363.22	2355.5	1000.4
332.54	1516.4	1230.6			
337.91	1516.4	1196.3	294.46	407.02	1398.9*
341.64	1516.4	1171.7	303.36	533.25	1361.6*
343.05	1516.4	1161.4	312.36	688.57	1324.2*
			319.47	833.39	1288.8*
299.03	1891.0	1393.2	326.02	986.00	1254.4*
306.31	1891.0	1364.2	332.99	1170.6	1215.2*
313.14	1891.0	1334.1	341.44	1428.6	1165.0*
319.12	1891.0	1306.4	347.27	1630.6	1124.6*
325.68	1891.0	1274.3	351.56	1793.1	1092.1*
333.38	1891.0	1233.7	355.44	1950.8	1060.0*
340.73	1891.0	1187.9	359.00	2105.1	1025.7*
346.41	1891.0	1147.9	362.72	2276.8	982.56*
350.45	1891.0	1114.7	364.73	2374.1	959.25*

* Saturated-liquid density.

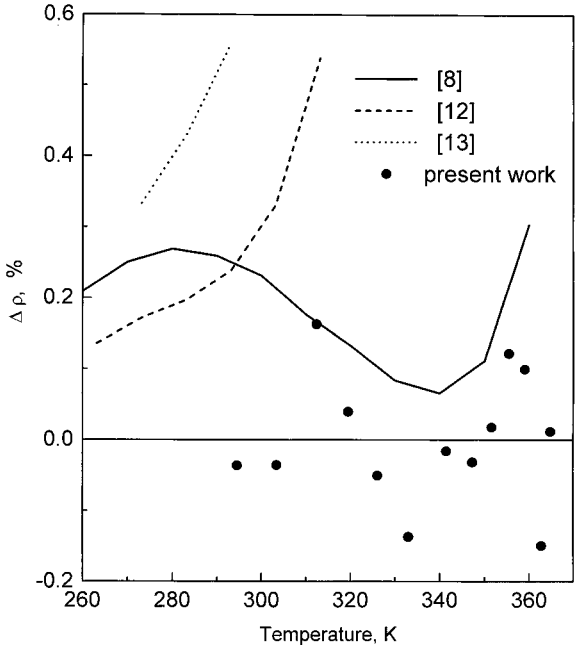

Fig. 3. Deviations of the experimental data for saturated liquid density from Eq. (5); $\Delta\rho = 100[\rho_l(\text{Ref.})/\rho_l(\text{Eq. (5)}) - 1]$.

of the rectilinear diameter. An extrapolation of ρ_d to the critical temperature gives the critical density $\rho_c = 591\ \text{kg}\cdot\text{m}^{-3}$. This value agrees with the value of $\rho_c = 584\ \text{kg}\cdot\text{m}^{-3}$ given in the handbook [7] to within extrapolation error. According to a recent view on the nature of critical phenomena, the asymptotic behavior of the liquid-vapor coexistence curve in the vicinity of the critical point is described by

$$(\rho_l - \rho_g) = B\varepsilon^{\beta} \tag{6}$$

where B is a constant. The value of the critical exponent β for the coexistence curve can be obtained as a slope of the dependence of $\ln(\rho_l - \rho_g)$ on $\ln(\varepsilon)$. Up to $\varepsilon \sim 0.2$ the dependence is rectilinear, to within the error, with a slope equal to 0.34 ± 0.01. This result is close to the non-classical value of β calculated from the Ising model, according to various methods, the calculated value lies in the range 0.31 to 0.34.

3.4. Speed of Sound

The speed of sound (u) was measured along isotherms from 273 to 393 K at increments of 10 K at pressures from 0.005 to 3.5 MPa and

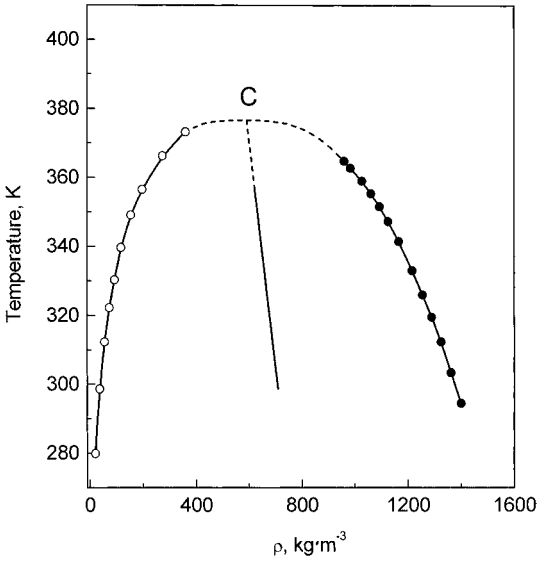

Fig. 4. Orthobaric densities of HFC-227ea along the liquid-vapor equilibrium line.

frequencies of 1.15 to 1.165 MHz. The results are given in Tables VI and VII and Figs. 5 and 6. There was no dispersion within the range of the thermodynamic parameters studied. A correlation of our measurements with the results of Ref. 1 has demonstrated that data from these studies agree within 0.1% on the isotherm at 273.15 K. Along the other isotherms the discrepancy is less than 0.25% up to 0.1 MPa and 0.15% at 0.1 to 0.5 MPa (Fig. 7). These discrepancies are less than the measurement errors.

To determine the speed of sound in the ideal-gas state (at $P \to 0$), the P-dependence of the speed of sound was approximated by polynomials of second or third order. The data obtained at $P < 0.1$ MPa and $P > 0.5$ MPa are ignored because of the possible influence of a velocity dispersion on the results at low pressure and to decrease sensitivity of the determination of u_0 to the functional form assumed for a $u(P)$-dependence, respectively. To estimate the ideal-gas molar heat capacity $C_p^0(T)$ of HFC-227ea with the help of a well-known thermodynamic ratio, the values of the ideal-gas sound speed $u_0(T)$ were used

$$C_p^0(T) = \frac{R}{\left(1 - \frac{RT}{\mu u_0^2}\right)} \tag{7}$$

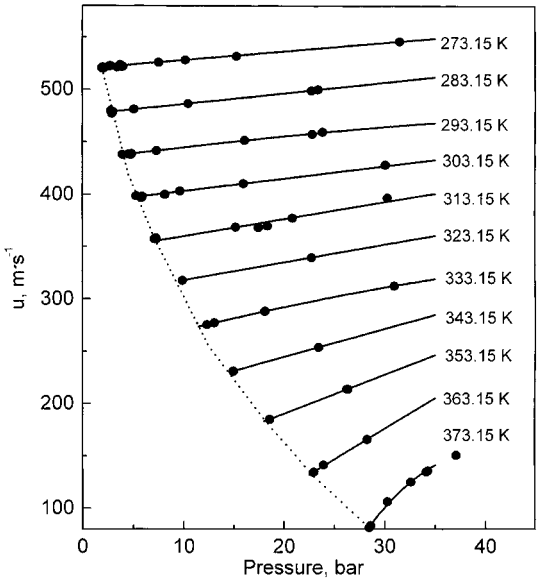

Fig. 5. Experimental sound-speed isotherms for liquid HFC-227ea.

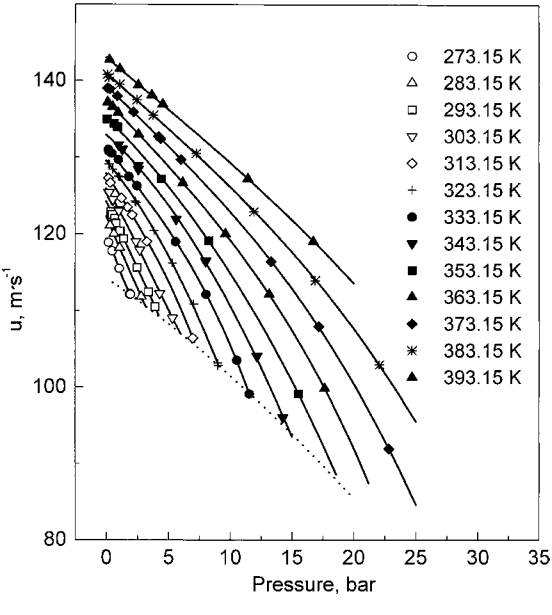

Fig. 6. Experimental sound-speed isotherms for vapor HFC-227ea.

Table VI. Experimental Speed of Sound in Liquid HFC-227ea

T (K)	P (kPa)	u (m·s^{-1})	P (kPa)	u (m·s^{-1})
273.15	192.9	520.5	199.2	521.2
273.15	264.0	522.4	277.3	522.5
273.15	341.4	521.3	367.0	522.6
273.15	373.9	523.6	753.3	525.8
273.15	1018.1	528.1	3199.7	545.9
283.15	278.4	480.0	278.9	479.8
283.15	299.9	478.8	508.7	481.3
283.15	1045.5	486.6	2273.6	498.9
283.15	2340.1	499.8		
293.15	394.8	437.9	451.6	438.2
293.15	484.5	438.7	732.0	441.5
293.15	1608.0	451.4	2282.4	457.8
293.15	2384.3	459.2		
303.15	528.8	398,6	562.4	397.9
303.15	589.5	398.0	812.3	400.0
303.15	963.1	403.3	1595.7	410.3
303.15	3006.3	427.9	4070.7	438.7
313.15	709.6	357.5	722.8	358.5
313.15	727.3	357.8	728.9	357.5
313.15	1745.4	368.4	1833.7	369.8
313.15	2082.8	377.3	3826.0	396.7
323.15	988.0	317.7	2274.3	339.6
333.15	1233.2	275.6	1305.3	277.3
333.15	1806.6	288.0	1812.2	288.3
333.15	3095.4	312.4		
343.15	1491.8	230.9	1492.7	231.2
343.15	1495.3	230.9	2344.6	253.8
353.15	1854.6	184.9	1855.3	185.1
353.15	2634.7	213.8	2635.1	213.7
363.15	2291.9	134.3	2295.3	134.7
363.15	2297.3	134.6	2391.4	141.4
363.15	2826.0	165.6		
373.15	2846.7	81.5	2860.6	83.4
373.15	3025.7	106.0	3257.4	125.0
373.15	3410.7	134.8	3706.1	150.6

The obtained data are correlated by the equation

$$C_p^0(T)/R = -6.08 + 0.11075T - 0.000122T^2 \tag{8}$$

Equation (8) describes the obtained data for $C_p^0(T)$ with an uncertainty of $\pm 0.08R$. Comparisons among our results and Refs. 1, 2, and 12 are shown in Fig. 8. Taking into account that the calculation of the heat capacity of polyatomic gases using speed-of-sound data with errors of 0.1% leads to

Table VII. Experimental Speed of Sound in Gaseous HFC-227ea

T (K)	P (kPa)	u ($m \cdot s^{-1}$)	P (kPa)	u ($m \cdot s^{-1}$)	P (kPa)	u ($m \cdot s^{-1}$)	P (kPa)	u ($m \cdot s^{-1}$)
273.15	17.9	118.9	47.3	117.8	104.7	115.5	170.9	113,3
273.15	185.7	112.1	189.1	112.2	193.5	112.1		
283.15	5.1	121.6	60.9	120.0	106.2	118.2	280.6	111.8
293.15	37.3	122.9	47.7	122.5	66.5	122.0	78.6	121.4
293.15	109.0	120.4	109.6	120.4	138.7	119.4	249.0	115.6
293.15	337.5	112.4	390.9	110.5				
303.15	19.9	125.4	50.9	124.4	53.4	124.5	101.0	123.1
303.15	101.3	123.0	237.4	119.0	269.0	117.9	429.4	112.2
303.15	23.5	125.4	532.2	109.0				
313.15	18.1	127.3	33.0	126,7	121.5	124.7	169.4	123,5
313.15	207.0	122.5	325.9	119,0	696.2	106.4		
323.15	20.1	129.1	25.8	129.1	54.0	128.4	99.3	127.5
323.15	109.1	127.4	232.6	124.3	239.1	124.1	383.7	120.4
323.15	532.4	116.2	704.1	110.8	899.3	103.1	900.2	102.8
333.15	17.6	131.0	20.8	130.8	43.9	130.5	97.7	129.7
333.15	180.3	127.5	246.2	126.3	555.8	119.0	803.5	112.1
333.15	1051.4	103.5	1153.2	99.1				
343.15	98.9	131.6	129.8	131.0	257.9	128.4	561.5	121.9
343.15	799.8	116.5	800.2	116.4	1215.7	104.0	1425.6	96.0
353.15	64.7	134,4	75.0	135.0	86.9	134,0	91.8	133.9
353.15	442.2	127.2	827.4	119.1	1551.5	99.1	1744.5	89,0
363.15	015.5	137.1	52.2	136.6	96.1	135.8	258.9	133.0
363.15	615.6	126.7	960.2	120.0	1315.0	112.1	1764.3	99.8
373.15	10.8	139.0	29.3	138.9	88.8	138.0	218.7	135.9
373.15	420.3	132.7	436.5	132.4	601.9	129.7	1331.6	116.4
373.15	1716.9	107.9	2282.5	91.9				
383.15	10.6	140.8	22.2	140.4	69.6	140,2	107.5	139.5
383.15	247.8	137.5	378.4	135.5	725.6	130.5	1191.1	122.9
383.15	1688.4	113.9	2207.2	102.9	2654.9	91.4	3035.4	79.2
393.15	26.3	142.7	59.7	142.4	109.1	141.5	258.5	139.4
393.15	365.6	138.1	452.5	136.9	1143.2	127.2	1672.1	119.0

errors in the molar heat capacity of 4 to 8%, our data and those from Ref. 1 are in good agreement. These values allowed us to conclude that the ideal-gas heat capacity of fluorinated derivatives of propane increases by $(8 \pm 0.5)\ J \cdot mol^{-1} \cdot K^{-1}$ per each fluorine atom. At the same time, a replacement of fluorine atoms by hydrogen atoms does not lead to noticeable changes in the slope of the temperature dependence of the heat capacity. A summary of the thermodynamic properties for HFC-227ea along the coexistence curve is given in Table VIII. Here the molar enthalpy of vaporization (ΔH_{vap}) is calculated using Eq. (1) for the saturated vapor pressure, Eqs. (5) for the densities of saturated vapor and liquid, and the Clausius–Clapeyron equation.

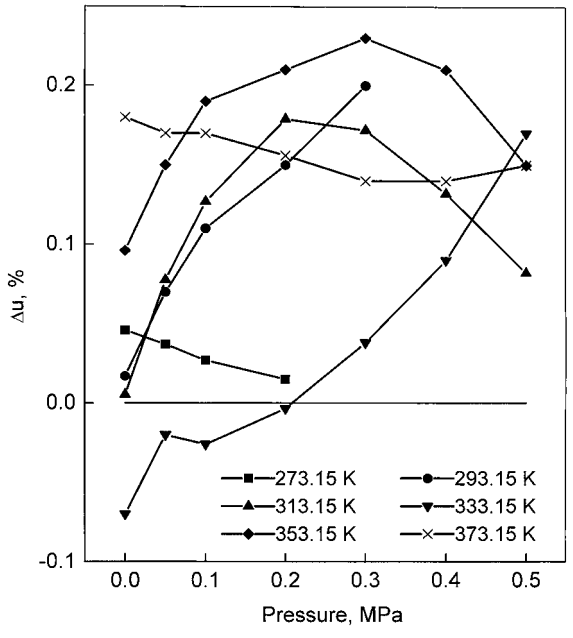

Fig. 7. Deviation of our sound-speed data from the data of Benedetto et al. [1]; $\Delta u = 100[u(\text{present work})/u(\text{Ref. 1}) - 1]$.

Table VIII. Thermodynamic Properties of HFC-227ea Along the Coexistence Curve

T (K)	P_s (kPa)	ρ_l (kg·m^{-3})	ρ_g (kg·m^{-3})	u_l (m·s^{-1})	u_g (m·s^{-1})	ΔH_{vap} (J·mole^{-1})
273.15	195.9	1480.3		521.0	112.0	
283.15	280.6	1443.2		478.7	111.8	
293.15	390.5	1404.3	29.4	437.7	110.5	20548
303.15	529.9	1363.0	40.7	398.0	109.0	19140
313.15	703.6	1318.6	55.5	357.4	106.4	17697
323.15	916.8	1270.1	74.6	316.4	103.0	16264
333.15	1175.2	1216.0	99.4	274.4	98.70	14821
343.15	1485.7	1153.7	131.8	230.8	93.60	13290
353.15	1856.4	1078.4	175.8	184.7	—	11550
363.15	2297.3	978.92	240.4	134.3	—	9297
373.15	2820.4	809.54	364.7	~77.0	—	5440

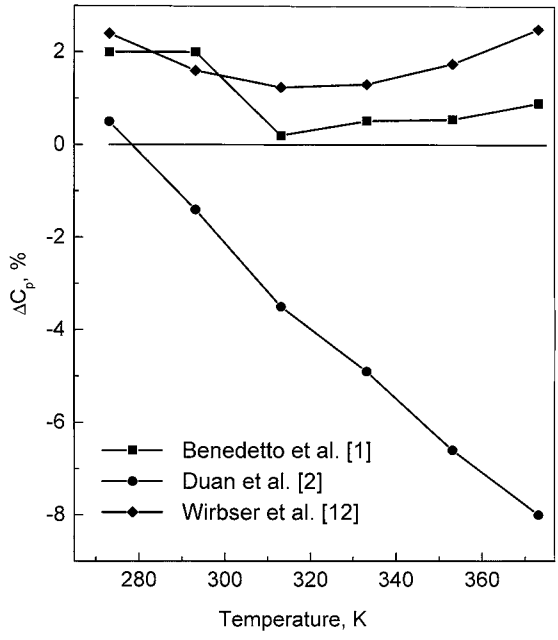

Fig. 8. Deviations of literature data for ideal-gas heat capacity of HFC-227ea from Eq. (8); $\Delta C_p = 100[C_p^0(\text{Ref.})/C_p^0(\text{Eq. (8)}) - 1]$.

ACKNOWLEDGMENTS

We gratefully acknowledge the financial support for this research from the Siberian Branch of the Russian Academy of Sciences (Grant IG-00-No. 47) and the Russian Foundation of Basic Research (Grants No. 01-02-16983, No. 01-03-32858).

NOMENCLATURE

C_p^0	heat capacity (J/mol)
P	pressure (kPa, MPa)
R	universal gas constant (J/mol K)
T	temperature (K)
u	speed of sound (m/s)
d	density (mol/l)
z	compressibility factor (dimensionless)

Greek Symbols

β	critical exponent (dimensionless)
ε	reduced temperature (dimensionless)
ρ	density (kg/m^3)
μ	molar mass (kg/mol)
ΔH_{vap}	molar enthalpy of vaporization (J/mol)

Subscripts

0	ideal-gas state
c	critical parameter
d	rectilinear diameter
g	vapor phase
l	liquid phase
s	liquid-vapor equilibrium

REFERENCES

1. G. Benedetto, R. M. Gavioso, R. Spagnolo, M. Grigiante, and G. Scalabrin, *Int. J. Thermophys.* **22**:1073 (2001).
2. Y. Y. Duan, L. Shi, M. S. Zhu, L. Z. Han, and C. Zhang, *Int. J. Thermophys.* (in press).
3. S. G. Komarov and V. A. Gruzdev, *Thermophys. Aeromech.* **6**:261 (1999).
4. S. G. Komarov and V. A. Gruzdev, *Thermophys. Aeromech.* **8**:467 (2001) (in Russian).
5. R. A. Khairulin and S. V. Stankus, *High Temp. High Press.* **32**:193 (2000).
6. A. L. Beyerlein, D. D. Des Marteau, S. H. Hwang, N. D. Smith, *ASHRAE Trans., Part 1* **99**:368 (1993).
7. V. N. Maksimov, V. G. Barabanov, I. I. Serushkin, V. S. Zotikov, I. A. Semerikova, V. P. Stepanov, N. G. Sagajdakova, G. I. Kaurova, *Industrial Fluorine-Organic Products* (Chemistry, St. Petersburg, 1996), pp. 82–83 (in Russian).
8. D. R. Defibaugh and M. R. Moldover, *J. Chem. Eng. Data* **42** (1):160 (1997)
9. M. Salvi-Narkhede, Bao-Huai Wang, J. L. Adcock, and W. A. Van Hock, *J. Chem. Thermodynam.* **24**:1065 (1992).
10. J. G. Hirschfelder, Ch. F. Churtiss, and R. B. Bird, *Molecular Theory of Gases and Liquids* (Wiley, New York, Champion and Hall Inc. London, 1954).
11. J. Patek, J. Klomfar, J. Prazak, and O. Sifner, *J. Chem. Thermodynam.* **30**:1159 (1998).
12. H. Wirbser, G. Brauning, J. Gurtner, and C. Ernst. *J. Chem. Thermodynam.* **24**:761 (1992).
13. V. N. Genrikh, V. A. Gruzdev, S. G. Komarov, and O. I. Verba, *Thermophys. Aeromech.* **7**:293 (2000).